Supplementary information

You get what you screen for: a benchmark analysis of leaf branch compost cutinase variants for polyethylene terephthalate (PET) degradation

Stefanie Fritzsche[1], Florentin Tischer[2], Wolfgang Peukert[2], Kathrin Castiglione[1*]

1 Institute of Bioprocess Engineering, Department of Chemical and Biological Engineering, Friedrich-Alexander-Universität Erlangen-Nürnberg, Paul-Gordan-Straße 3, 91052 Erlangen, Germany
2 Institute of Particle Technology, Department of Chemical and Biological Engineering, Friedrich-Alexander-Universität Erlangen-Nürnberg, Cauerstraße 4, 91052 Erlangen, Germany

*Corresponding author: kathrin.castiglione@fau.de

Surrogate substrates

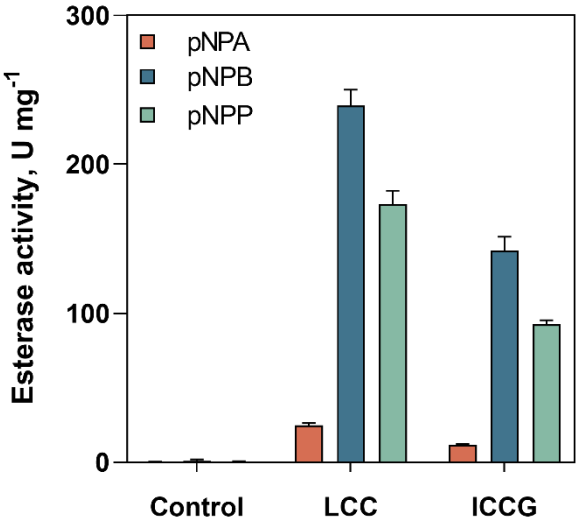

Figure S1: Enzymatic hydrolysis of pNPA, pNPB and pNPP using different enzyme variants at 37 °C. Esterase activity was calculated by measuring the absorbance at 405 nm. Each bar represents the mean value of three independent replicates ± SD.

The esterase activities of the well-characterised enzymes LCC and ICCG were compared with three different nitrophenyl esters as substrates. The activities towards the different substrates differed by a factor of up to 10 under the same reaction conditions (Figure S1). The highest activities were measured for the medium chain pNPB. Compared to the ICCG variant, the wild type showed a significantly higher total esterase activity for all substrates.

PET Materials

Different substrates were used for PET hydrolysis. There were two different types of fibres, both from post-industrial waste and similar in physical properties such as fibre strength, but different in colour and therefore in the dyes added (Figure S2).

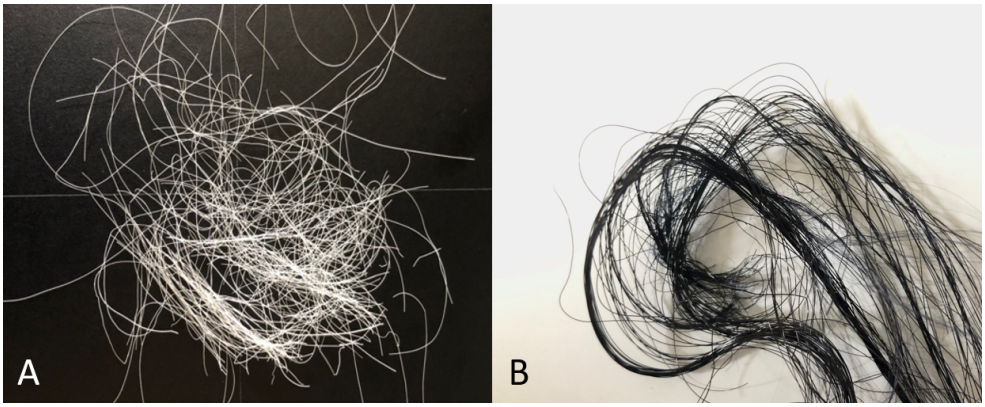

Figure S2: Post-industrial PET textile fibres in white (A) and black (B). For use in PET hydrolysis, the fibres were shortened to a length of about 1 cm.

Characterisation of PET samples regarding thermal and physical properties

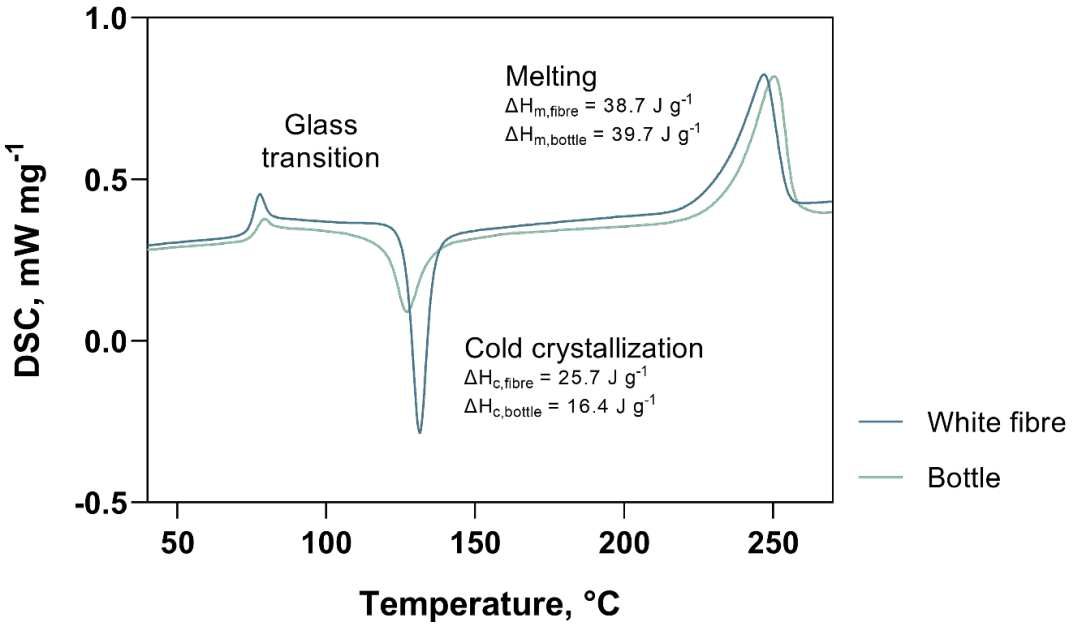

Figure S3: DSC profile of white textile fibres and comminuted bottle PET in a temperature range from 20 to 280 °C. The peaks correspond to the glass transition, cold crystallization and melting with the respective enthalpies.

DSC showed similar glass transition temperatures for bottle PET and fibres of 74.7 and 74.2 °C, respectively (Figure S3). In addition to the melting peaks, peaks for cold crystallization were

observed for both materials, which can be traced back to a rapid cooling during the initial manufacturing process. In the case of the fibres, the cold crystallization was much more prominent, indicating a significantly higher amorphous amount. Ultimately, the degree of crystallization determined by DSC was 9 % for the fibres and 16 % for the bottle PET.

To assess the morphology of the surface, the fibres diameters and to visualize the degradation process, SEM was used (Figure S4 and Figure S5). A flat surface was observed for the fibres with a diameter of 100 – 150 µm (Figure S4).

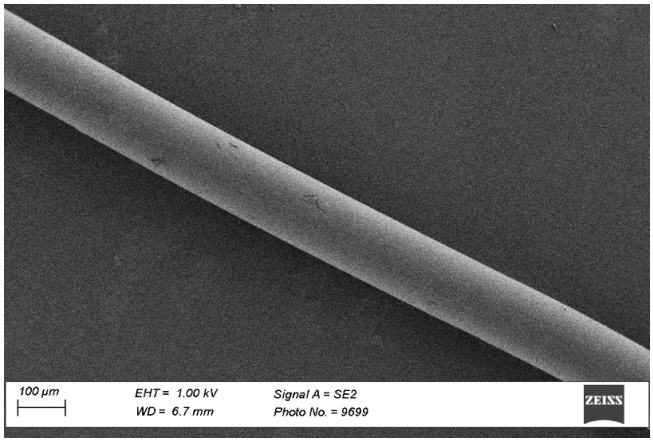

Figure S4: SEM image of a white PET fibre to evaluate surface morphology and fibre diameter.

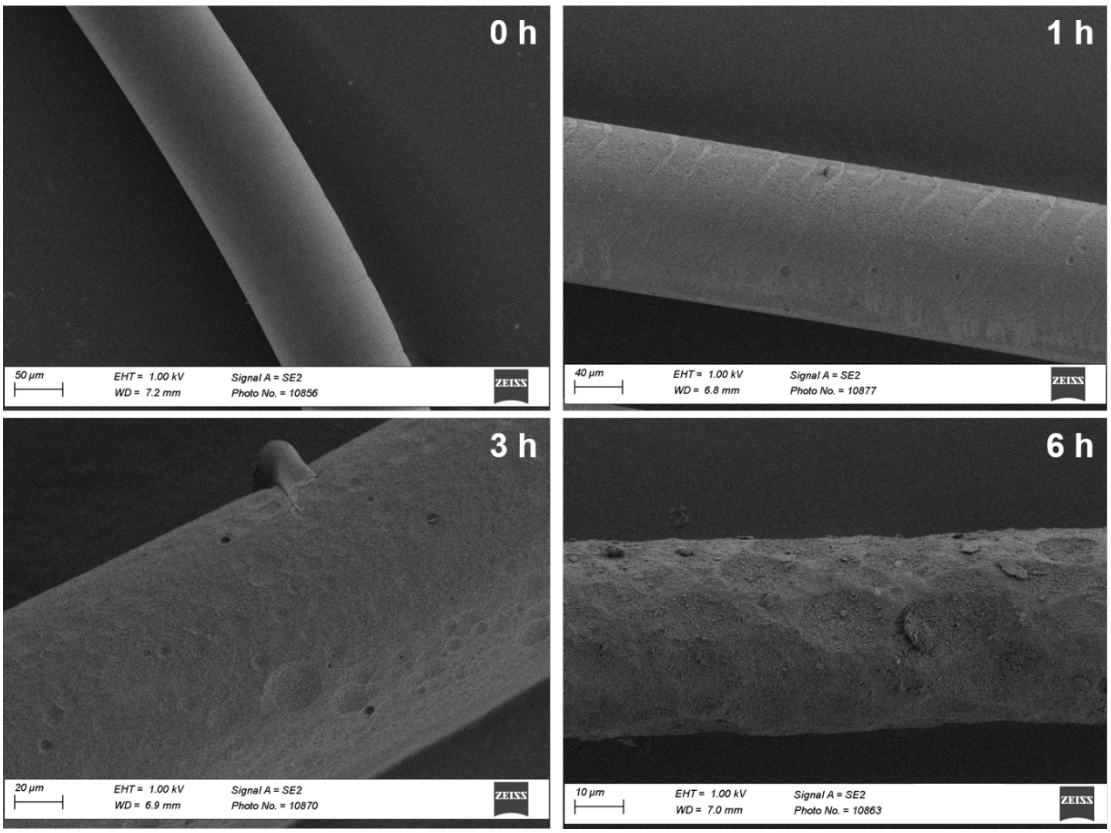

Figure S5: SEM images of the white PET fibres before hydrolysis and after enzymatic degradation for 1 h, 3 h and 6 h.

The particle size distribution recorded for the bottle powder resulted in an $x_{50,3}$ of 573 µm (Figure S6). Based on gas adsorption (BET theory), the specific surface area of the fibres and ground PET powder was determined (Table S1).

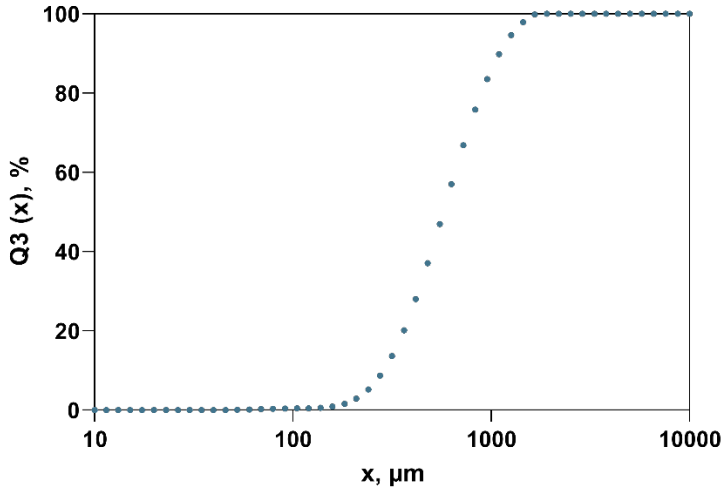

Figure S6: Particle size distribution curve Q3(x) as a function of the particle size x obtained for the bottle powder.

Table S1: Physical properties of the PET materials mainly used in this work. The specific surface area S_M was calculated based on gas adsorption (BET theory). For comminuted PET bottles a particle size distribution could be determined by laser diffraction, while for the PET fibres the average diameter was assessed by SEM.

Material	Specific surface area S_M, $m^2\ g^{-1}$	Particle size distribution $x_{50,3}$, µm	Average diameter, µm
Bottle powder	0.059	573	-
PET fibres	0.211	-	130 ± 20

Molecular docking and identification of relevant loops

Regions for loop swapping were identified based on the enzyme-ligand complex obtained from molecular docking. Promising regions for amino acid exchange were loops close to the substrate binding groove and/or the active site. Four loops A - D were selected, for which Table S2 provides further positioning information.

Table S2: Loops identified by molecular docking of a 4PET substrate to the protein crystal structure using AutoDock Vina for loop swapping, including the corresponding amino acid positions.

Loop	Amino acid positions
A	L 187 – V 202
B	A 207 – A 219
C	L 237 – A 244
D	N 246 – A 250

HPLC profiles for product characterization and reaction monitoring

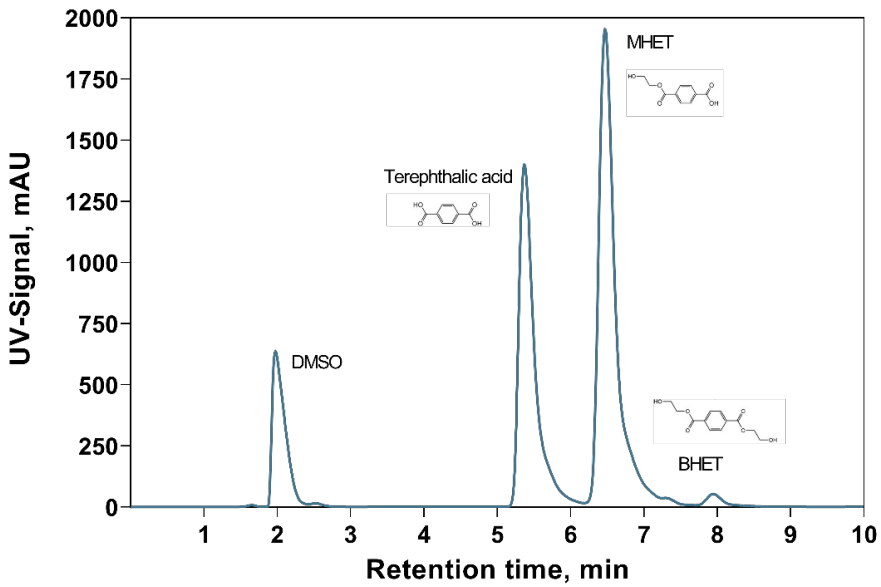

Figure S7: HPLC profile of a hydrolysis sample after 3 h of reaction time. Hydrolysis of white PET fibres was performed in miniaturized stirred reactors at 72 °C with 1 mg g_{PET}^{-1} enzyme addition and 100 mM phosphate buffer. RP-HPLC analysis was performed on a C18 Nucleodur column with 20 % acetonitrile : 79.9 % H_2O : 0.1 % formic acid as mobile phase at a flow rate of 0.6 mL min^{-1}. UV signal was measured at 240 nm.

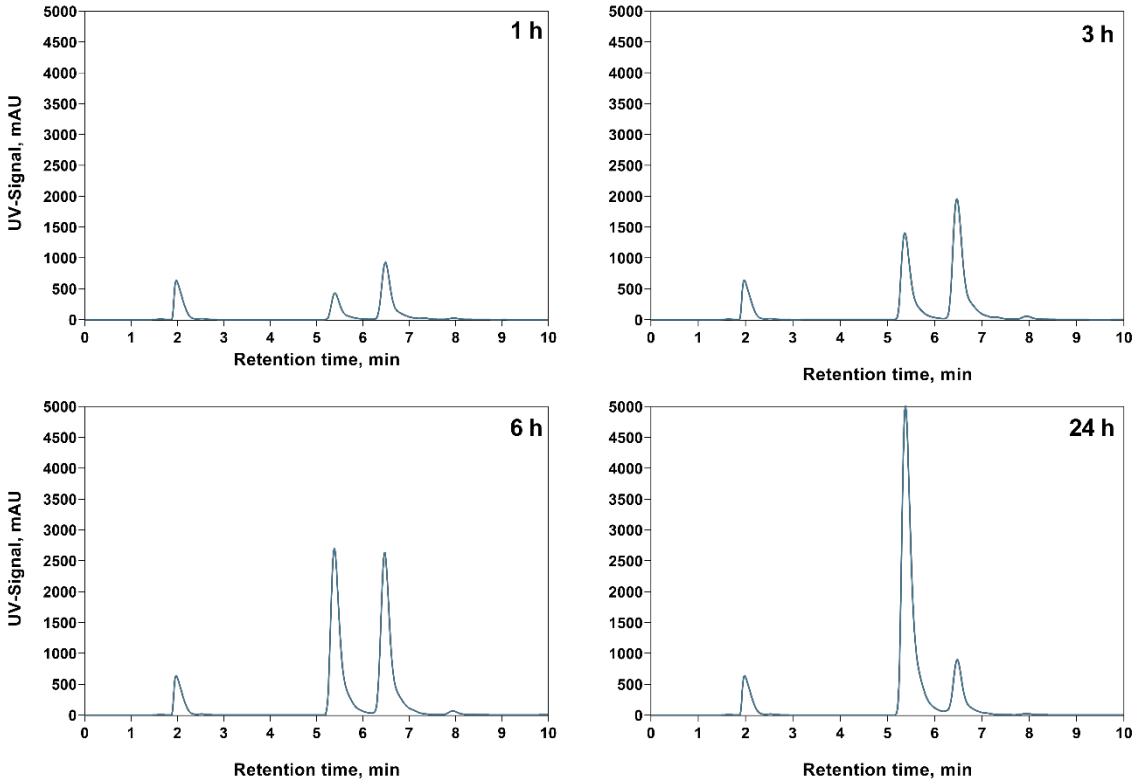

Figure S8: HPLC profiles of hydrolysis products over time. Samples were analysed by RP-HPLC after 1, 3, 6 and 24 h. Any necessary dilutions of the samples were already taken into account. Hydrolysis of white PET fibres was performed in miniaturized stirred reactors at 72 °C with 1 mg g_{PET}^{-1} enzyme addition and 100 mM phosphate buffer. RP-HPLC analysis was performed on a C18 Nucleodur column with 20 % acetonitrile : 79.9 % H_2O : 0.1 % formic acid as mobile phase at a flow rate of 0.6 mL min^{-1}. UV signal was measured at 240 nm.

As shown in Figure S7, all the products of PET hydrolysis - terephthalic acid, MHET and BHET - could be clearly identified and quantified by HPLC. Even with a short analysis time of only 10 minutes, a good resolution of the peaks could be achieved. Monitoring the product release over time, it could be clearly seen that in the beginning mainly MHET was released (for pH 8), while over time it shifted to the hydrolysis of PET and intermediates to the final product terephthalic acid. In the end, mainly terephthalic acid was detected (Figure S8).

Relation between enzyme variant and substrate specificity

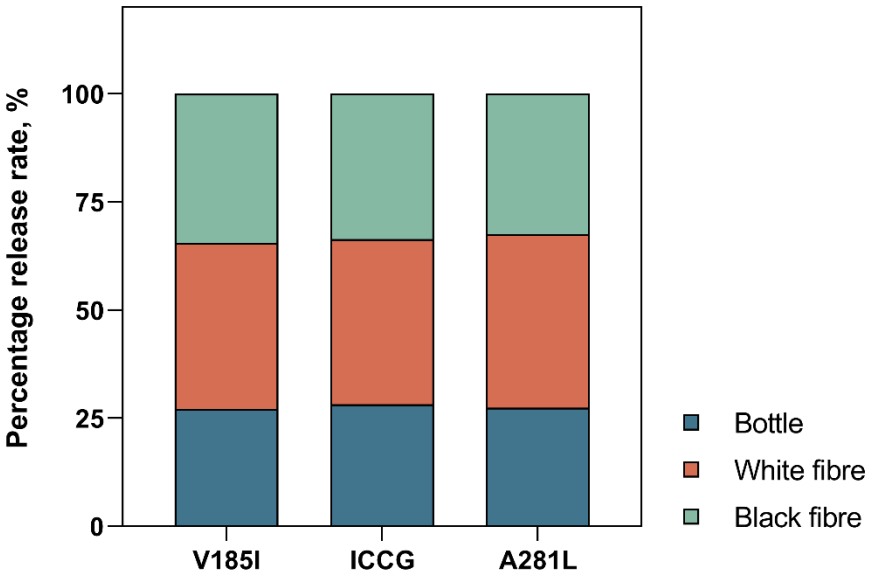

Figure S9: Relative product releases for the substrates bottle, white and black fibres using different enzyme variants. Hydrolysis was performed in miniaturized stirred reactors at 72 °C with 1 mg g_{PET}^{-1} enzyme addition and 100 mM phosphate buffer.

The product release rates for the different three substrates of a good (V185I) and a poor performing variant (A281L) as well as the reference enzyme (ICCG) were compared. As shown in Figure S9, there were no significant differences, i.e. there was no clear improvement or decline in the individual mutants when using a particular substrate.

PET hydrolysis over time in miniaturised stirred tank reactors

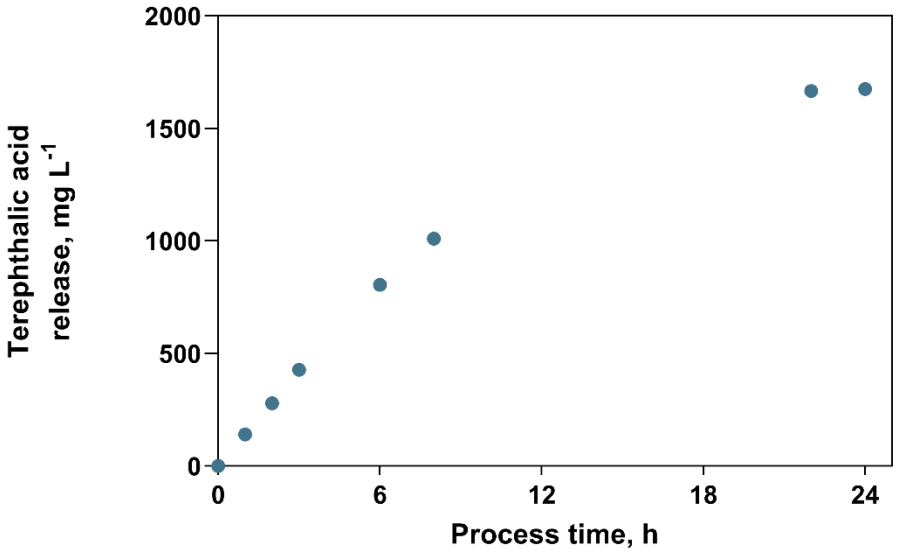

Figure S10: Release of terephthalic acid over 24 hours of hydrolysis. White PET fibres were used for hydrolysis in miniaturized stirred reactors at 72 °C with 1 mg g_{PET}^{-1} enzyme addition and 100 mM phosphate buffer, pH 10.

During hydrolysis, an almost linear course of terephthalic acid release was initially observed as seen in Figure S10. After 8 hours, the release rate slowly decreased before a final terephthalic acid concentration of 1676 mg L^{-1} was observed after 24 hours. Considering the maximum possible terephthalic acid release, this corresponds to a conversion of 97 %, which can be considered as complete. The process time for a complete PET degradation was thus less than 24 h process time.

Evaluation of activity versus stability

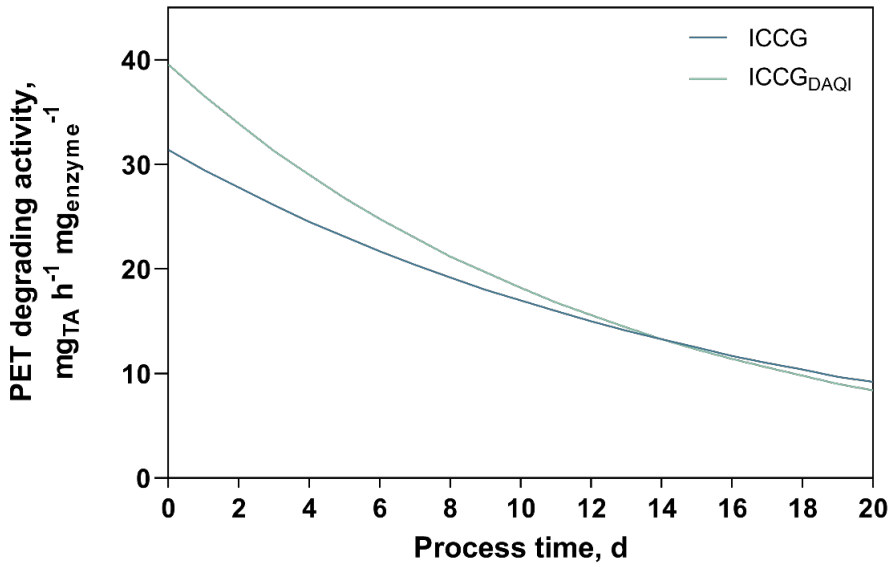

Figure S11: Calculated PET degrading activity considering the thermal stability and the resulting inactivation rates of the two enzyme variants over time up to the break-even point. PET degrading activity A over time t was calculated starting from the initial activities A_0 and the thermal inactivation rates k determined by the half-lifes of the variants: $A = A_0 \cdot e^{k \cdot t}$.

Starting from a product release of 31 mg_{TA} mg_{enzyme}^{-1} h^{-1} for ICCG and a 26 % higher PET degrading activity for $ICCG_{DAQI}$, the calculated activity steadily decreases taking the thermal inactivation into account (Figure S11). The activity of DAQI consistently exceeds that of ICCG in the first days of the process, despite the lower thermal stability. The break-even point is reached only after 14 days. From this point on, the activity of the ICCG exceeds that of the DAQI variant due to the higher thermal stability.

Comparing the degradation activity of two enzymes at their respective optimum temperatures

As shown in Figures S12 and S13, the release of the hydrolysis target product terephthalic acid was compared for the two respective optimum temperatures of the enzymes IsPETase and the $ICCG_{DAQI}$ variant. At 72 °C the expected release of terephthalic acid by $ICCG_{DAQI}$ was obtained, whereas for IsPETase only a maximum concentration of 19 mg L^{-1} and thus almost no activity was observed. At 40 °C, which should be the optimum temperature for IsPETase, the activity of $ICCG_{DAQI}$ was also severely reduced, as is known at lower temperatures, but a better PET degradation rate was also here found for $ICCG_{DAQI}$ compared to IsPETase. For white and black fibres (data not shown) the same effects were observed.

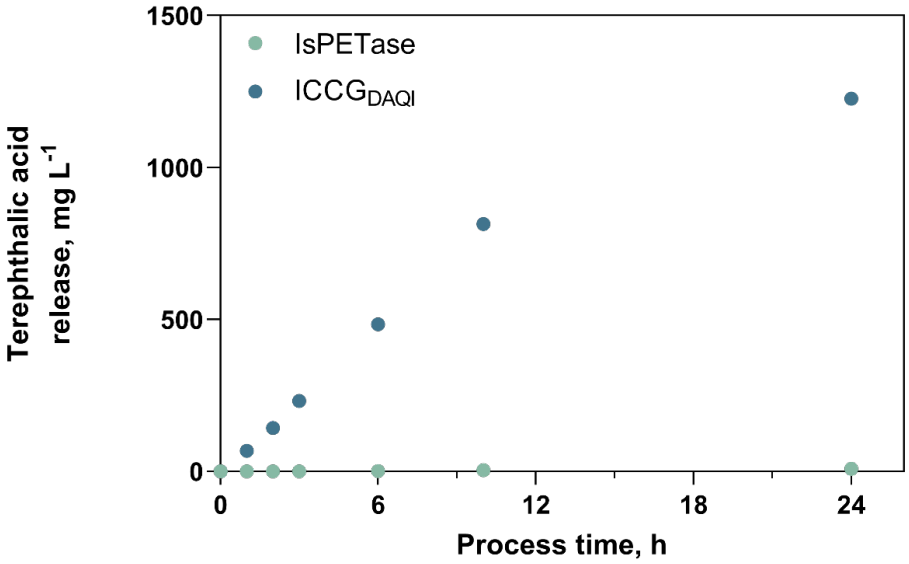

Figure S12: Release of terephthalic acid over 24 hours of hydrolysis. Comminuted PET bottle powder was used for hydrolysis in miniaturized stirred reactors at 72 °C with 1 mg g_{PET}^{-1} enzyme addition and 100 mM phosphate buffer, pH 8.

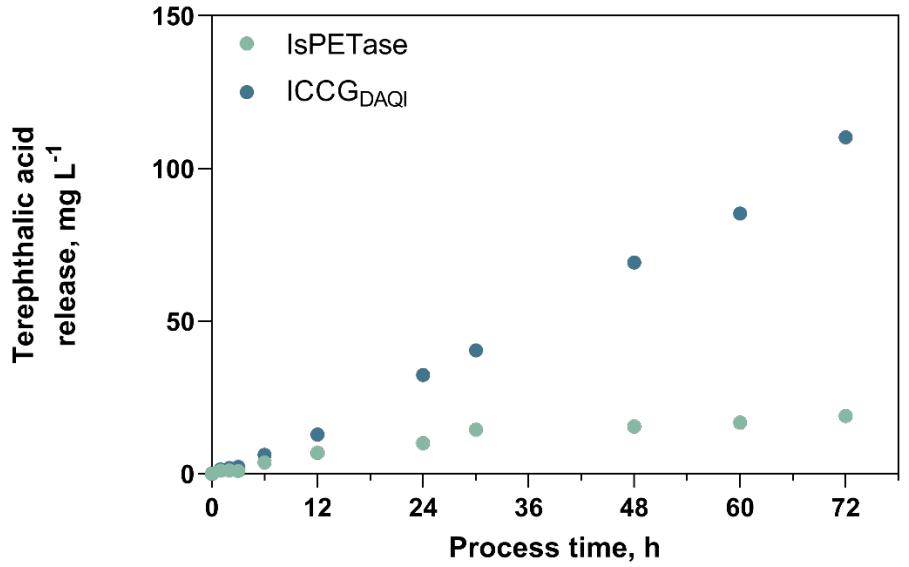

Figure S13: Release of terephthalic acid over 72 hours of hydrolysis. Comminuted PET bottle powder was used for hydrolysis in miniaturized stirred reactors at 40 °C with 1 mg g_{PET}^{-1} enzyme addition and 100 mM phosphate buffer, pH 8.

Table S3: List of PCR primers used in this work for amino acid exchanges.

Primer	Sequence (5' – 3')	
	forward	reverse
S146D	CTCGGATCACTGGTACGCAGGTAGTTC	CAGTGATCCGAGCGCCGTTCG
S146R	CTCGGACGACTGGTACGCAGGTAG	CAGTCGTCCGAGCGCCGTTC
G170A	CGGTGCGACCCTGCGTATTGCAGAACAAAACC	GGGTCGCACCGCCACCCATAGAATGACC
S180D	CCCGGATCTGAAAGCGGCTGTCCCGC	CAGATCCGGGTTTTGTTCTGCAATACGCAGG
V185I	GGCTATTCCGCTGACCCC GTGGCACAC	CAGCGGAATAGCCGCTTTCAGGCTCGGG
T192L	GGCACCTGGATAAAACGTTTAATACCAGTGTCCC	CGTTTTATCCAGGTGCCACGGGGTCAG
D193N	CACACCAACAAAACGTTTAATACCAGTGTCCCGG	CGTTTTGTTGGTGTGCCACGGGGTCAGC
D193Q	CACACCCAGAAAACGTTTAATACCAGTGTCCCGG	CGTTTTCTGGGTGTGCCACGGGGTCAGC
A207C	GGCTGCGAAGCTGACACCGTGGCGC	GCTTCGCAGCCAACAATCAGCACCGGGACAC
F243S	CGCACAGCGCTCCGAATAGCAACAATGCGGCC	GAGCGCTGTGCGATGCGTTGCACAGTTCGACG
A244C	CTTCTGCCCGAATAGCAACAATGCG	CGGGCAGAAGTGCGATGCGTTATCC
N246F	CTCCGTTTAGCAACAATGCGGCCATTTCCG	GCTAAACGGAGCGAAGTGCGATGCGTTATC
A251L	CCCGCTGCTGTCCGACTTCCGCACCAATAATCG	GGACAGCAGCGGGTCGTTCACATTACACAGG